

are categorized into conjugated and nonconjugated biradicals, and the former is further divided into Kekulé and non-Kekulé systems.⁹ In contrast to a large number of investigations for non-Kekulé and nonconjugated biradicals, the electronic structure of singlet biradicals with Kekulé structures has been less thoroughly examined. Although the most extensive studies in the Kekulé singlet biradical have been performed on Chichibabin's hydrocarbon,¹⁰ the potential high reactivity and flexible molecular framework make a definitive electronic structure still open for discussion. Recently, we have prepared and characterized a stable phenalenyl-based¹¹ Kekulé singlet biradical **1b** with a rigid structure, and have clarified a prominent feature of strong *intermolecular* spin-spin interactions.¹²

Herein, we will report the synthesis and single-molecular electronic structure of a novel Kekulé polycyclic hydrocarbon with substantial biradical character. Our newly designed molecule **2** has a naphthoquinoid structure along with two phenalenyl rings. The singlet biradical index γ of **2** is expected to be larger than that of **1** (γ of **1a** = 30%), because two benzene rings appear in the biradical resonance structure **2'** in contrast to only one in **1**. The CASSCF(2,2)/6-31G//RB3LYP/6-31G** calculation of **2a** gave the LUMO occupation number of 0.504, from which the γ value was determined to be 50%, according to the NOON (natural orbital occupation number) analysis.¹³ Spin density distribution was estimated by using a broken-symmetry (BS)

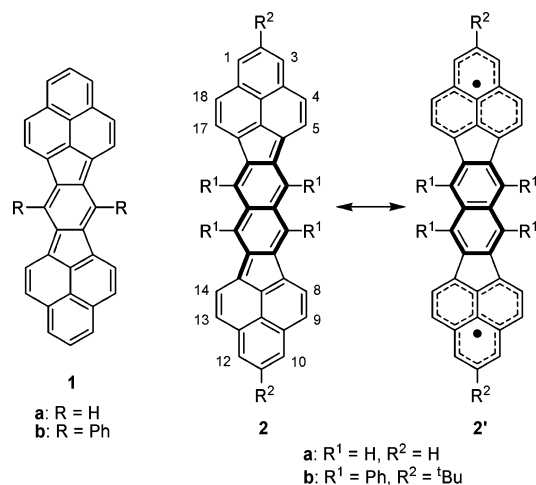


Figure 1. Phenalenyl-based singlet biradicals.

UB3LYP/6-31G** method, which indicated large spin density on two phenalenyl rings with antiparallel spins retaining the characteristic spin distribution pattern of phenalenyl radical (Figure 2). Thus the electronic structure of **2** in a ground state is best represented by the resonance of Kekulé and biradical forms as shown in Figure 1.

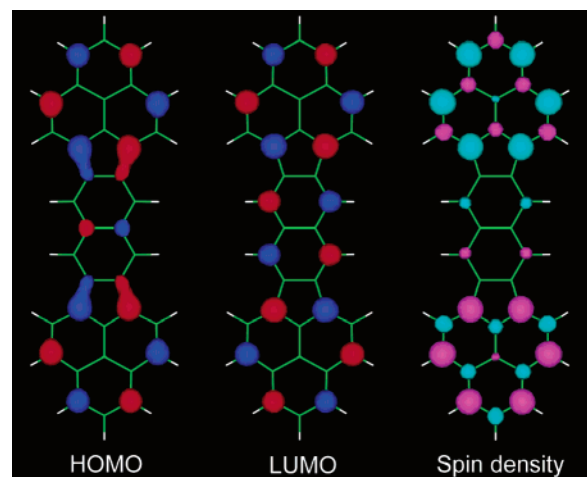


Figure 2. HOMO, LUMO, and spin density of **2a**. Red and blue surfaces represent positive and negative signs of molecular orbitals calculated with a RB3LYP/6-31G** method, respectively. Light blue and light red surfaces represent α and β spin densities, respectively.

Because most polycyclic aromatic compounds suffer from low solubility, we have decided to introduce phenyl and *tert*-butyl substituents on the rings of **2a**. The synthetic procedure for the derivative **2b** is shown in Scheme 1. The starting

(13) (a) Döhnert, D.; Koutecký, J. *J. Am. Chem. Soc.* **1980**, *102*, 1789–1796. (b) Jung, Y.; Head-Gordon, M. *ChemPhysChem* **2003**, *4*, 522–525. For the calculation details of **2a**, see the Supporting Information.

(2) (a) Montgomery, L. K.; Huffman, J. C.; Jurczak, E. A.; Grendze, M. *P. J. Am. Chem. Soc.* **1986**, *108*, 6004–6011. (b) Rajca, A.; Rajca, S. *J. Am. Chem. Soc.* **1996**, *118*, 8121–8126.

(3) (a) Ullman, E. F.; Osiecki, J. H.; Boocock, D. G. B.; Darcy, R. *J. Am. Chem. Soc.* **1972**, *94*, 7049–7059. (b) Alies, F.; Luneau, D.; Laugier, J.; Rey, P. *J. Phys. Chem.* **1993**, *97*, 2922–2925. (c) Frank, N. L.; Clérac, R.; Sutter, J.-P.; Daro, N.; Kahn, O.; Coulon, C.; Green, M. T.; Golhen, S.; Ouahab, L. *J. Am. Chem. Soc.* **2000**, *122*, 2053–2061. (d) Ziesel, R.; Stroh, C.; Heise, H.; Köhler, F. H.; Turek, P.; Clauser, N.; Souhassou, M.; Lecomte, C. *J. Am. Chem. Soc.* **2004**, *126*, 12604–12613.

(4) Kanno, F.; Inoue, K.; Koga, N.; Iwamura, H. *J. Am. Chem. Soc.* **1993**, *115*, 847–850.

(5) (a) Brook, D. J. R.; Fox, H. H.; Lynch, V.; Fox, M. A. *J. Phys. Chem.* **1996**, *100*, 2066–2071. (b) Brook, D. J. R.; Yee, G. T. *J. Org. Chem.* **2006**, *71*, 4889–4895.

(6) (a) Sugimoto, T.; Sakaguchi, M.; Ando, H.; Tanaka, T.; Yoshida, Z.; Yamauchi, J.; Kai, Y.; Kanehisa, N.; Kasai, N. *J. Am. Chem. Soc.* **1992**, *114*, 1893–1895. (b) Shultz, D. A.; Boal, A. K.; Farmer, G. T. *J. Am. Chem. Soc.* **1997**, *119*, 3846–3847. (c) Rebmann, A.; Zhou, J.; Schuler, P.; Rieker, A.; Stegmann, H. B. *J. Chem. Soc., Perkin Trans. 2* **1997**, 1615–1617.

(7) Shultz, D. A.; Kumar, R. K. *J. Am. Chem. Soc.* **2001**, *123*, 6431–6432.

(8) Kikuchi, A.; Ito, H.; Abe, J. *J. Phys. Chem. B* **2005**, *109*, 19448–19453.

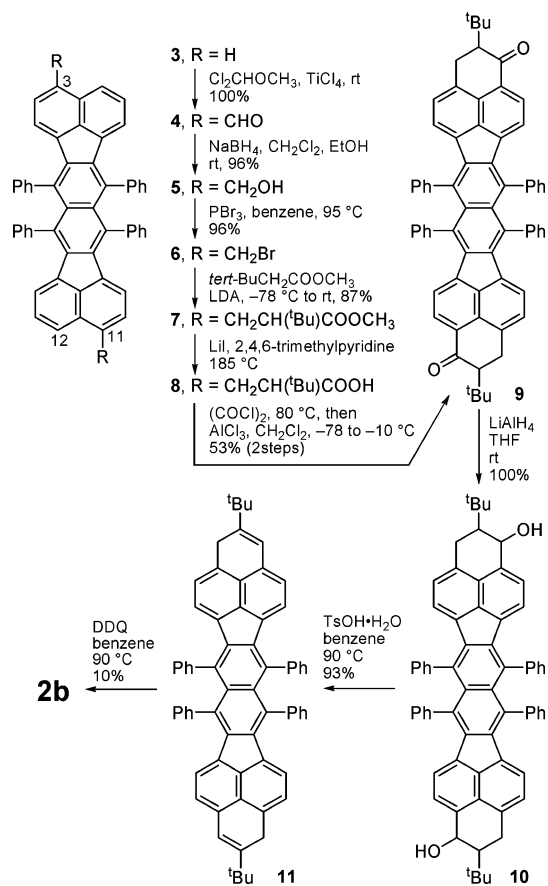
(9) Borden, W. T. In *Diradicals*; Borden, W. T., Ed.; Wiley: New York, 1982; in preface, which indicates biradicals include carbenes, non-conjugated, conjugated non-Kekulé, and anti-aromatic. We used the term “conjugated Kekulé” instead of “anti-aromatic” for wider application of the categorization.

(10) Platz, M. S. In *Diradicals*; Borden, W. T., Ed.; Wiley: New York, 1982; pp 201–209. Reference 2a also summarizes the results of investigations.

(11) Our recent works of the phenalenyl system: (a) Morita, Y.; Aoki, T.; Fukui, K.; Nakazawa, S.; Tamaki, K.; Suzuki, S.; Fuyuhiko, A.; Yamamoto, K.; Sato, K.; Shiomi, D.; Naito, A.; Takui, T.; Nakasuji, K. *Angew. Chem., Int. Ed.* **2002**, *41*, 1793–1796. (b) Nishida, S.; Morita, Y.; Fukui, K.; Sato, K.; Shiomi, D.; Takui, T.; Nakasuji, K. *Angew. Chem., Int. Ed.* **2005**, *44*, 7277–7280. (c) Suzuki, S.; Morita, Y.; Fukui, K.; Sato, K.; Shiomi, D.; Takui, T.; Nakasuji, K. *J. Am. Chem. Soc.* **2006**, *128*, 2530–2531.

(12) Kubo, T.; Shimizu, A.; Sakamoto, M.; Uruichi, M.; Yakushi, K.; Nakano, M.; Shiomi, D.; Sato, K.; Takui, T.; Morita, Y.; Nakasuji, K. *Angew. Chem., Int. Ed.* **2005**, *44*, 6564–6568.

Scheme 1. Synthetic Procedure for 2b



compound **3**, which was obtained according to the reported procedure,¹⁴ was converted to diformyl derivatives as a mixture of 3,11- and 3,12-isomers.¹⁵ Carboxylic acid derivatives **8** were prepared in five steps. Intramolecular Friedel–Crafts cyclization of the acyl chloride of **8** with AlCl₃ gave diketones **9**, which were reduced and subsequently dehydrated to afford dihydro compound **11**. The dehydrogenation of **11** with DDQ provided the target compound **2b** as dark violet plates. The solid **2b** was found to be stable at room temperature in air for a couple of days. The molecular structure was determined by the X-ray crystallography of a single crystal of **2b** (Figure 3).¹⁶ The crystal of **2b** included toluene solvent molecules. The main core rings have planar geometries, and phenyl groups are perpendicular to the plane. There are no appreciable π – π contacts between molecules (Figure S1).

The electronic absorption spectrum of **2b** in a hexane/dichloromethane (49:1, v/v) solution gave an intense low-energy band at 865 nm ($\epsilon = 78\,433$) as shown in Figure 4 (red line). To assess the band with respect to biradical

(14) Neudorff, W. D.; Schulte, N.; Lentz, D.; Schlüter, A. D. *Org. Lett.* **2001**, *3*, 3115–3118.

(15) Individual isomers were not isolated for further transformations because both isomers could lead to a single compound **2b**.

(16) Crystal data for **2b**: monoclinic, *P*2₁/*n* (no. 14), *a* = 16.109(7) Å, *b* = 9.036(3) Å, *c* = 19.383(8) Å, $\beta = 94.544(7)^\circ$, *V* = 2812.5(1) Å³, *Z* = 2, *T* = 150 K, *R*1(*wR*2) = 0.070 (0.184) for 370 parameters and 3823 independent reflections, GOF = 1.14.

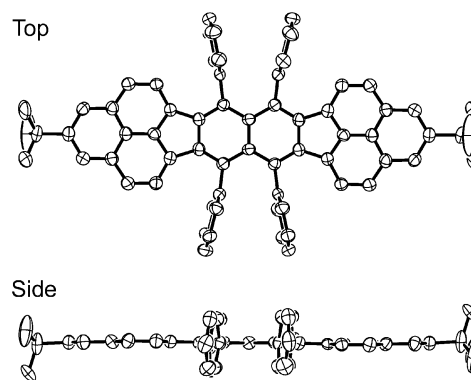


Figure 3. ORTEP drawings of **2b** at the 50% probability level. Hydrogen atoms and toluene molecules were omitted for clarity.

character, we performed time-dependent (TD) B3LYP calculations, which were summarized in Table 1. The broken-

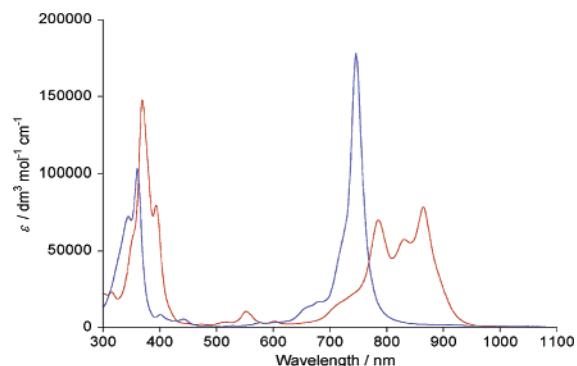


Figure 4. Solution absorption spectra of **1b** (blue) and **2b** (red).

symmetry UB3LYP calculations reproduce quite well the transition energies (ΔE) and oscillator strengths (*f*) observed in **1b** and **2b**, whereas the RB3LYP calculations show smaller ΔE and much larger *f* values than the observed ones. In general, a TD–RDFT (Restricted DFT) calculation

Table 1. Observed and Calculated Transition Energies (ΔE) and Oscillator Strengths (*f*) of **1** and **2**

	1a, 1b		2a, 2b	
	ΔE (eV)	<i>f</i>	ΔE (eV)	<i>f</i>
observed	1.66	0.65 ^c	1.43	0.63 ^c
RB3LYP ^a	1.59	0.86	1.38	1.03
UB3LYP ^b	1.61	0.60	1.46	0.55

^a Time-dependent RB3LYP/6-31G** calculation at the RB3LYP/6-31G** optimized geometry of **1a** and **2a**. ^b Time-dependent UB3LYP(BS)/6-31G** calculation at the UB3LYP(BS)/6-31G** optimized geometry of **1a** and **2a**. ^c The oscillator strengths were obtained by the integration of the absorbance in the range of 560–830 nm for **1b** and 630–1000 nm for **2b**.

provides an optical gap in good agreement with the experiment for most closed-shell compounds.¹⁷ A single-determinant restricted calculation is, however, insufficient for the description of the ground state of singlet biradicals.^{18a} In contrast, a broken-symmetry UDFT (Unrestricted DFT) method is suitable for the approximate description of the singlet biradical electronic structure.^{18b} Better agreement of the UB3LYP results with the observed transition energies implies the biradical contribution to the ground state in **1b** and **2b**.¹⁹ The oscillator strengths f are more informative for biradical character. The RB3LYP, which have no biradical contribution, predicts the larger f for the more expanded conjugation system **2a** than for **1a**,²⁰ in clear contrast to the experimental result. The RB3LYP calculations of **1a** and **2a** afford fully delocalized frontier orbitals (see ref 12 and Figure 2), whereas the UB3LYP gives the MO pictures localizing on one side of the molecule (Figure S2). In the UB3LYP method, the wave function in the HOMO occupies regions in space different from that in the LUMO as a result of the biradical contribution, and the intensity-determining integrals for the transition would be small. The theoretical and experimental f values of **2** are smaller than those of **1**. These UV results along with the TD-UB3LYP calculations imply **2b** is a Kekulé system with larger biradical character, that is a more spin-localized system,²¹ compared to **1b**.

The cyclic voltammogram of **2b** showed four reversible redox waves: $E_2^{\text{ox}} = +0.26$, $E_1^{\text{ox}} = -0.13$, $E_1^{\text{red}} = -1.17$, and $E_2^{\text{red}} = -1.55$ (V vs Fc/Fc⁺, see Figure S3). From the difference between the first oxidation and reduction potentials, the electrochemical HOMO–LUMO gap is estimated to be 1.04 eV, which is 0.11 eV smaller than that of the tetra-*tert*-butyl derivative of **1a**.²² The smaller energy gaps are consistent with the larger biradical character of **2b**, because a HOMO–LUMO gap is closely related to the promotion of electrons from HOMO to LUMO. Admixing a doubly excited configuration ${}^1\Phi_{\text{H,H-L,L}}$ into a ground state leads to a strong static correlation between two unpaired electrons, and consequently the system has pronounced singlet biradical character.

The weakening spin–spin coupling originating from the small HOMO–LUMO gap leads to thermal excitation to a triplet state. A powdered sample of **2b** showed an increasing

susceptibility above 250 K in a SQUID measurement (Figure S4). The singlet–triplet energy gap ($\Delta E_{\text{S-T}}$) was estimated to be ~ 1900 K, which was consistent with the theoretically calculated value of 2250 K using the B3LYP/6-31G** method, and was smaller than that of **1b**. The $\Delta E_{\text{S-T}}$ is, however, much larger than those in most non-Kekulé and nonconjugated singlet biradicals, indicating an adequate antiparallel spin–spin interaction. We could not discern ESR signals of the triplet species in the powdered **2b**, since a $\Delta M_s = 1$ peak of a monoradical impurity (peak-to-peak width, $\Delta H_{\text{pp}} = 1.4$ mT) would obscure the triplet species signal which should have a small D value (~ 1.6 mT) according to the distance between the centers of phenalenyl rings. The monoradical impurity would originate from partial oxidation or hydrogenation of **2b**. In a toluene solution of **2b** at room temperature, the ESR spectrum consisted of 15 sharp peaks centered at $g = 2.0029$. Double integral of the signal indicated the monoradical concentration of $\sim 2\%$.^{23,24}

The CD₂Cl₂ solution of **2b** showed no ¹H-NMR signals of the main core rings at +20 °C. Upon cooling, progressive line sharpening of the signals on the ring protons was observed. Even at –100 °C, however, the signals were slightly broad (Figure S6). Thermally excited triplet species are responsible for this signal broadening. Although a similar behavior has also been observed in **1b**, sharp signals are obtained at –30 °C.¹² The signal broadening of **2b** at lower temperature supports the smaller $\Delta E_{\text{S-T}}$ compared to **1b**.

In conclusion, the experimental assessment of **2b** strongly supported the larger biradical character as compared to **1b**. The UV spectra combined with the TD-UB3LYP calculations suggested the more localized spin structure in **2b** than **1b**, while the SQUID and NMR measurements indicated **2b** still has sufficient spin–spin coupling in antiparallel manner. This bifunctional character, that is spin localization and pairing, is consistent with the intermediate biradical character ($y = 50\%$) calculated with the CASSCF method. Currently, we are investigating an intermolecular interaction of a Kekulé singlet biradical with the intermediate biradical character.

Acknowledgment. This work is partly supported by Mitsubishi Chemical Corporation Fund, PRESTO-JST, and a Grant-in-Aid for Scientific Research (17550034) and in priority areas “Application of Molecular Spins” (Area No. 769) from the Ministry of Education, Science, Sports, and Culture, Japan.

Supporting Information Available: The detailed synthetic procedure of **2b**, and crystallographic data in CIF format. This material is available free of charge via the Internet at <http://pubs.acs.org>.

OL062604Z

(23) The hyperfine coupling constants determined were 0.510 (4H) and 0.157 mT (2H), which could be assigned to α and β protons on the phenalenyl ring, respectively (Figure S5). The parent phenalenyl radical has hyperfine coupling constants of 0.63 and 0.18 mT for α and β protons, respectively. See: Gerson, F. *Helv. Chim. Acta* **1966**, *49*, 1463–1467.

(24) A reviewer pointed out a possibility that the monoradical impurity might be responsible for the increasing magnetic susceptibility above 250 K. However, the closest π – π overlap on the main core ring of **2b** between the molecules is over 5 Å, which would not lead to a sizable J value.

(17) (a) Heinze, H. H.; Görling, A.; Rösch, N. *J. Chem. Phys.* **2000**, *113*, 2088–2099. (b) Dierksen, M.; Grimme, S. *J. Phys. Chem. A* **2004**, *108*, 10225–10237.

(18) (a) The biradical contribution like **2'** to the ground state requires an appropriate electron–electron repulsion effect (static electron–electron correlation), which can be calculated by using a multiconfigurational wave function such as a CASSCF method. (b) With the spin-symmetry broken method, the static correlation is simulated, and the ground state bears biradical character.

(19) For a successful application of the UB3LYP(BS) calculation for UV transition of singlet biradical states, see: Gao, Y.; Liu, C.-G.; Jiang, Y.-S. *J. Phys. Chem. A* **2002**, *106*, 5380–5384.

(20) Oscillator strength f is known to be related to the square of a transition dipole moment, and the dipole moment is represented by $\sum e\mathbf{r}$, where \mathbf{r} is the dipole length. Thus the RB3LYP would produce the larger f for **2a** with a longer molecular skeleton.

(21) We used the term “localized” for describing the spin structure of the conjugated Kekulé biradical. The term originates from the distribution pattern of wave functions where the highest occupied α and β molecular orbitals are localized in different regions of the molecule.

(22) Ohashi, K.; Kubo, T.; Masui, T.; Yamamoto, K.; Nakasuiji, K.; Takui, T.; Kai, Y.; Murata, I. *J. Am. Chem. Soc.* **1998**, *120*, 2018–2027.